

Crown Ether Annelated Tetrathiafulvalenes. 2

T. K. Hansen,^{*,†} T. Jørgensen,[†] F. Jensen,[†] P. H. Thygesen,[†] K. Christiansen,[†]
M. B. Hursthouse,[‡] M. E. Harman,[‡] M. A. Malik,[‡] B. Girmay,[§] A. E. Underhill,[§] M. Begtrup,[⊥]
J. D. Kilburn,^{||} K. Belmore,[⊙] P. Roepstorff,[∇] and J. Becher[†]

Department of Chemistry, Odense University, DK-5230 Odense M, Denmark, School of Chemistry and Applied Chemistry, PO Box 912, Cardiff, CF1 3TB, U.K., Department of Chemistry, University College of North Wales, Bangor LL57 2UW Gwynedd, Wales, U.K., Danish Pharmaceutical University, Universitetsparken 2, DK-2100 Copenhagen, Denmark, Department of Chemistry, University of Southampton, Highfield, Southampton, SO9 5NH, U.K., Department of Chemistry, University of Alabama, P.O. 870336, Tuscaloosa, Alabama 35487, and Department of Molecular Biology, Odense University, DK-5230 Odense M, Denmark

Received August 28, 1992

A synthetic procedure leading to derivatives of tetrathiafulvalene (TTF) incorporating polyether chains of various lengths, some nitrogen analogs, and a 2,6-bis(methylene)pyridine analog has been developed. These compounds possess cage-type structures which were confirmed by X-ray crystallography in four cases, two of which are reported herein for the first time. Structural and electronic features of these cage molecules were correlated to oxidation potentials by the use of semiempirical methods (MNDO-PM3). An investigation of the alkali metal ion affinity using PDMS revealed that these compounds are poor ligands. Finally, in one case, protonation of the core TTF was studied by NMR.

Introduction

Organic π -donors and their cation radical salts have been studied extensively in recent years because of their potential as molecular conductors and superconductors.¹ The most successful systems studied to date incorporate the tetrathiafulvalene (TTF) moiety. We have been investigating the possibility of incorporating these electroactive TTF units into metal-binding macrocyclic structures in hopes that these materials would exhibit altered electrochemical properties in the presence of suitable cations, leading to novel organic conducting materials. In addition, these molecules are examples of redox-active macrocycles and could potentially serve as metal cation sensors. We have previously reported our preliminary findings in this area,² and more recently we reported the full details³ of our studies on planar TTF derivatives with various crown ethers attached at each end of the TTF

unit. These materials were prepared by the triethyl phosphite-mediated coupling of thiones (such as 9-13, Figure 1), which in turn were prepared as 1:1 adducts from the reaction of dithiolate 1 with various polyether bromides. These compounds showed significant shifts in their oxidation potentials in the presence of metal cations, as indicated by cyclic voltammetry measurements. We have also found that the reactions between dithiolate 1 and suitable bis electrophiles, aside from giving 1:1 adducts (monomers), also give larger macrocyclic systems, particularly 2:2 adducts (dimers). On treatment with triethyl phosphite, these dimers undergo intramolecular coupling to produce novel TTF cage molecules (Figure 2). These molecules are constitutionally the same as the planar TTF crown ethers prepared by intermolecular coupling of the corresponding 1:1 adducts, but in this case the macrocycle chains run from one end of the TTF unit to the other. For these compounds the TTF unit is generally distorted out of planarity, with the degree of distortion reflecting the length of the macrocyclic chain. Despite this distortion, however, in some cases the TTF units exhibit two reversible one-electron oxidations in cyclic voltammetry experiments. Prior to this work there were only a few examples in the literature of similarly distorted TTF's; compound 26 (Table III) and two other related macrocyclic TTF systems all showed one irreversible oxidation⁴ peak in the CV. In this paper we report the full experimental details on the synthesis of a series of these cage molecules, including several new examples which have increased the range of molecules in this series, and report for the first time the crystal structures of 20 and 21. In principle, these cage molecules could also bind to metal cations to produce redox-active ligands, but they have also allowed us to probe the effects on the oxidation potentials as a function of the degree of distortion and of the through-space effects of the heteroatoms in the macrocyclic chain, through a comparison of the X-ray crystal structures of 20, 21, 23, 25, and 26, and by the use of semiempirical methods using MNDO-PM3. We have also examined the alkali metal ion affinity of the cages using plasma desorption mass

[†] Department of Chemistry, Odense University.

[‡] School of Chemistry and Applied Chemistry.

[§] University College of North Wales.

[⊥] Danish Pharmaceutical University.

^{||} University of Southampton.

[⊙] University of Alabama.

[∇] Department of Molecular Biology, Odense University.

(1) For reviews on TTF see: (a) Coleman, L. B.; Cohen, M. J.; Sandman, D. J.; Yamagishi, F. G.; Garito, A. F.; Heeger, A. J. *Solid State Commun.* 1973, 12, 1125. (b) Ferraris, J.; Cowan, D. O.; Walatka, V.; Perlstein, J. H.; *J. Am. Chem. Soc.* 1973, 95, 498. (c) Williams, J. M.; Wang, H. H.; Emge, T. J.; Geiser, U.; Beno, M. A.; Leung, P. C. W.; Carlson, K. D.; Thorn, R. J.; Schultz, A. J.; Whangbo, M.; *Prog. Inorg. Chem.* 1987, 51 (review). (d) Schukat, G.; Richter, A. M.; Fanghänel, E. *Sulfur Rep.* 1987, 155.

(2) For previous communications covering aspects related to the work presented here see: (a) Becher, J.; Hansen, T. K.; Malhotra, N.; Bojesen, G.; Bowadt, S.; Varma, K. S.; Girmay, B.; Kilburn, J.; Underhill, A. E. *J. Chem. Soc., Perkin Trans. 1* 1990, 175. (b) Jørgensen, T.; Becher, J.; Hansen, T. K.; Christiansen, K.; Roepstorff, P.; Larsen, S.; Nygaard, A. *Adv. Mater.* 1991, 3, 486. (c) Girmay, B.; Kilburn, J. D.; Underhill, A. E.; Varma, K. S.; Hursthouse, M. B.; Harman, M. E.; Becher, J.; Bojesen, G. *J. Chem. Soc., Chem. Commun.* 1989, 1406.

(3) *Crownether Annelated Tetrathiafulvalenes (I)*; Hansen, T. K., Jørgensen, T., Stein, P. C., Becher, J. *J. Org. Chem.* 1992, 57, 6403.

(4) (a) Röhrich, J.; Wolf, P.; Enkelmann, V.; Müllen, K. *Angew. Chem.* 1988, 100, 1429. (b) For a more recent example of a "bent" TTF derivative see also: Bertho-Thoraval, F.; Robert, A.; Souizi, A.; Boubekeur, K.; Batail, P. *J. Chem. Soc., Chem. Commun.* 1991, 843. **Note Added in Proof.** See also: Röhrich, J.; Müllen, K. *J. Org. Chem.* 1992, 57, 2374.

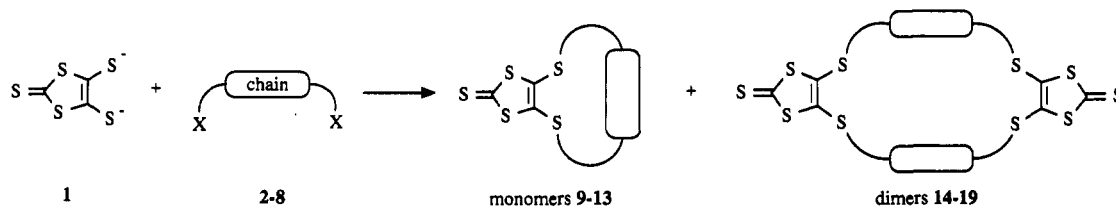


Figure 1. 1 used as the disodium salt, see Experimental Section.

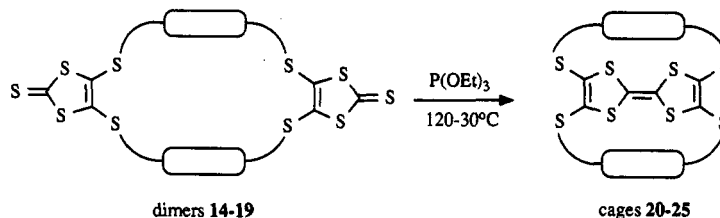


Figure 2.

Table I

starting material	yields (isolated), %					
	monomers		dimers		cages	
2	9:	65	14:	22	20:	19
3	10:	60	15:	25	21:	22
4	11:	61	16:	25	22:	<1
5	12:	87	-	-	-	-
6	13:	1	17:	18	23:	32
7	-	0	18:	16	24:	23
8	-	0	19:	95	25:	22

spectrometry (PDMS), and we have found that these compounds are relatively poor ligands. An interesting feature of these cage compounds, however, is that they are readily protonated to form cationic species which can be examined in detail using NMR and we report herein the full details of one example of this procedure.

Results and Discussion

The synthesis of the dimeric precursors necessary for intramolecular coupling to tetrathiafulvalene cages is outlined in Figure 1 and the yields are given in Table I. The method utilizes disodium salt 1 as a general starting material which can be conveniently generated from 4,5-bis(benzoylthio)-1,3-dithiole-2-thione by treatment with base.⁵ In reactions with polyether dibromides 2-4 we obtained mixtures of monomers and dimers, which could be optimized to yield 60-65% of monomer or 20-25% of dimer. However, as previously described,³ the reaction of 1 with 5 produced monomer 12 exclusively in 87% yield. In the nitrogen-containing starting materials 6-8 it is striking that 19 was formed in very high yield (95%) from 8, compared to the far lower yields of 17 and 18 obtained when 6 and 7 were employed. This result might reflect self-condensation of 6 and 7, differences in the flexibility

of the chain, as well as differences in reactivity. Work with 6 and 7 was severely hampered by the highly toxic nature of these mustard compounds, which must be handled with utmost care.

In all cases but one, the dimers coupled in an intramolecular fashion when heated in xylene in the presence of triethylphosphite. Yields were 19-32%,⁶ and the products crystallized, in most cases, after evaporation of the xylene. Usually, intermolecular coupling of thiones to TTF's took place rapidly in neat triethylphosphite,⁷ however, in some cases (e.g., 15), the reaction mixture polymerized and formed a transparent gel, which could be washed with methanol, leaving a totally insoluble unidentified pale orange material. These problems were circumvented by using xylene as the reaction medium. Surprisingly, the coupling of 16 afforded cage 22 in very poor yield (sufficient for MS), precluding full characterization of 22. However, we were able to observe (on the TLC plates) that 22 is clearly yellow-red, in contrast to the other cages which are almost colorless. CPK models indicate that the polyether

(5) (a) Steimecke, G.; Sieler, H.; Kirmse, R.; Hoyer, E.; *Phosphorus Sulfur* 1979, 7, 49. (b) Varma, K. S.; Bury, A.; Harris, N. T.; Underhill, A. E. *Synthesis* 1987, 837.

(6) The yields of this type of reaction in general are often 30-50% for intermolecular couplings; thus, these intramolecular couplings are below the low end of the range. In order to understand the low yields we chromatographed the mother liquor after collection of cages 20-22. We obtained an orange oil which by mass spectrometric analysis was assumed to be the Arbuzov product shown in Figure 9.

(7) Yoneda, S.; Kawase, T.; Inaba, M.; Yoshida, Z. *J. Org. Chem.* 1978, 4, 596.

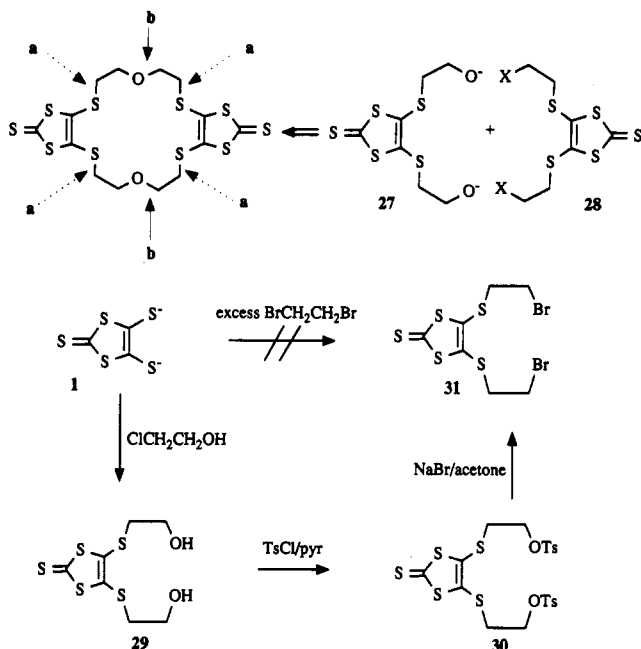


Figure 3. 1 used as the disodium salt, see Experimental Section.

chains in **22** are long enough to allow planarity of the TTF unit, which consequently has the normal color of a TTF derivative, in contrast to the more or less "bent" derivatives **20** and **21**. CPK models also indicate that **20** has a very rigid structure with a highly distorted TTF core and practically no central cavity. (This is probably the case for all derivatives with short connecting chains.) Complexation of metal cations consequently seems unlikely in the case of **20**, whereas **21** is a far more flexible molecule and definitely possesses a central cavity. However, it appears that the cavity is not well-defined, as the molecule can adopt many conformations with a wide variety of central cavity sizes, even some with the donor atoms outside the cavity. This topic will be discussed further in the crystallographic section.

Although the synthesis outlined above (Figures 1 and 2) did afford the desired compounds, we hoped to obtain better yields via different routes. As indicated in Figure 3, the dimer **14** is constructed via formation of four bonds which are denoted "a" in Figure 3. This approach obviously allows the formation of many higher oligomers and inherently produces workup problems and low yields.

Assuming that the two compounds **27** and **28** suggested by retrosynthesis were available, we anticipated that the same compound **14** could be produced by the formation of only two new bonds (denoted "b"). Under high dilution conditions this process could lead to better yields of **14**. For this purpose we developed a synthesis for dibromide **31** via the alkylation⁸ of **1** with chloroethanol to **29** and tosylation to the relatively unstable **30**, which could be converted in good yield to dibromide **31**. However, all attempts to cause the bromine atoms to undergo nucleophilic substitution using oxygen or nitrogen nucleophiles⁹ proved unsuccessful. We obtained two principle products as a result of these attempts (Figure 4), the elimination

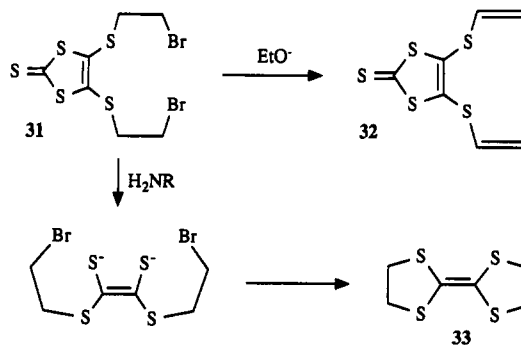


Figure 4.

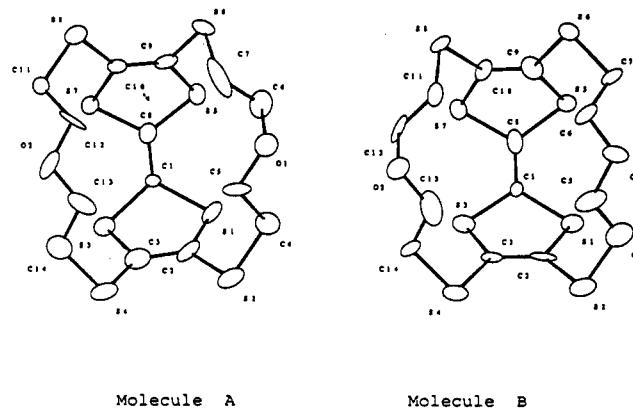


Figure 5. General view of the structures of the two crystallographically independent molecules of **20** with atom numbering scheme.

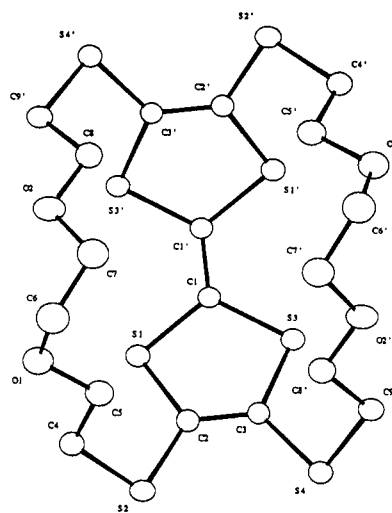


Figure 6. The molecule of **21** viewed along the crystallographic 2-fold axis, which relates the primed atoms to the unprimed ones of the same number.

product **32** and the tetrathioethylene **33**, which probably results from nucleophilic opening of the 1,3-dithiole ring. Preparation of compound **29** from **1** was recently described by Kozzov et al.⁸

The structures of cages **20** and **21** have been determined by X-ray crystallography, the former with low precision due to poor crystal quality. The main features of the two structures are clear, however. The unit cell of **20** contains two crystallographically independent molecules shown in Figure 5 (a and b) and their centrosymmetric counterparts; the structure of a single molecule of **21** is shown in Figure 6.

The molecule **21** possesses a crystallographic 2-fold axis of symmetry passing through the midpoint of the central

(8) After the completion of our work, related work describing the intermediate **29** was published by: (a) More, A. J.; Bryce, M. R. *J. Chem. Soc., Chem. Commun.* 1991, 1639. (b) Kozzov, E. S.; Yurchenko, A. A.; Tozmachev, A. A.; Nechitaino, L. A.; Ignatev, N. V. *Zh. Org. Chim.* 1990, 26, 377.

(9) Under carefully controlled conditions we have observed that **31** undergoes nucleophilic substitution with the sulfur nucleophile **1** in good yield. These results will be published at a later stage.

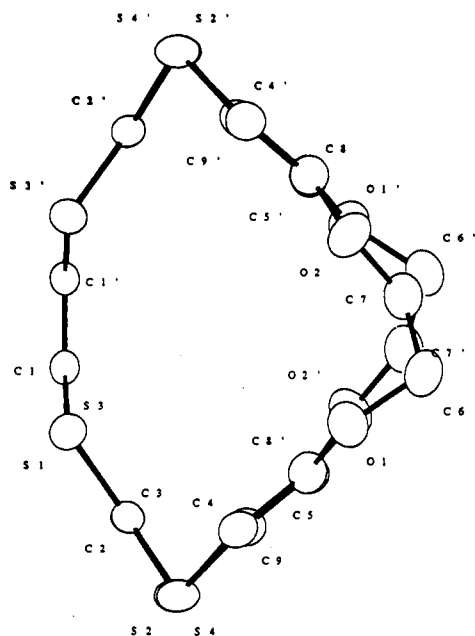


Figure 7. A sideways view of the molecule of 21 showing the bending of the two 5-membered rings away from the central $S_2C=CS_2$ moiety.

$C(1)-C(1')$ bond and perpendicular to the mean plane of the tetrathia fragment. The bond lengths between a given pair of atoms are consistent with the sums of their atomic radii and bond orders. The $C(1)-C(1')$ and $C(2)-C(3)$ double bonds [1.347(7) and 1.344(6) Å] and all the single bonds show only minor deviations from the expected values. The $S-C(sp^2)$ distances [1.743(5)–1.771(1) Å] are shorter by 0.07 Å than the $S-C(sp^3)$ distances [1.819(6) and 1.823(6) Å], which is consistent with the difference in atomic radii for sp^2 and sp^3 carbons. It is notable, however, that the angles involving chemically equivalent atoms show some variations [for example, the tetrahedral angles at the C atoms vary from 106.4(4) to 114.5(5)°], which may be attributed to the presence of strain within the molecule.

Although the molecular geometry parameters for 20 obtained from the present work are not very accurate, the salient features of the structure can be easily discerned. In contrast with 21, none of the two independent molecules of 20 possesses any 2-fold axial or any other symmetry, and as is evident from Figure 5 (a and b), the two $-CH_2-CH_2OCH_2CH_2-$ groups linking a pair of exocyclic S atoms on the two dithiole rings in each molecule are oriented quite differently. The chemically equivalent bond lengths and angles in the two molecules are comparable with the corresponding values in 21. The presence of the external chains results in significant deformation (bending) of the central TTF unit, with pyramidalization at the fulvalene carbons, folding of the dithiole rings along the $S\cdots S$ vector and bending of the exocyclic C–S bonds. This is well demonstrated in Figure 7, which depicts a sideways view of 21 along the $S(1)\cdots S(3)$ vector. Additionally, the magnitude of the deformations can be seen from the least-squares plane for the tetrathia part of the molecule and the dihedral angles formed between the central $C=C$ bond and the envelope of the dithiole ring, the envelope flap and the body of the ring, and the body and the external $S-C-C-S$ unit. These data, presented in Table II for 20 and 21 as well as two related structures, clearly demonstrate that the strain deformations, comparable in compounds 20, 23, 25, and 26, but significantly larger than in 21, are correlated with the different external bridge lengths. The

intermolecular distances in both compounds are comparable with the usual van der Waals contacts.

The oxidation potentials of 20 and 21 were measured using cyclic voltammetry, and the results are listed in Table III along with data^{2,3} obtained from other cage molecules 23, 25, and 26 (determined under comparable conditions). Though the five compounds all possess a distorted TTF structure, the oxidation potentials vary by about 1 V, a surprisingly high variation. A simple explanation of these data is to assume a correlation between the "bending" of the TTF unit and the oxidation potential. A larger bending would produce a less efficient conjugation and destabilize a radical cation. As is evident from the data in Table III there is no simple connection between the oxidation potential and the distortion of the TTF moiety (measured as the out-of-plane "bending" of the central double bond).

When attempting the rational design of compounds it is helpful to develop a deeper understanding of the factors influencing the various properties. For this reason we have performed MO calculations on the cage compounds 20, 21, 23, 25, and 26. The size of these systems precludes the use of ab initio methods, and consequently we have relied on the MNDO-PM3 method introduced by Stewart.¹⁰ In each case the geometries were fully optimized.¹¹ Ionization potentials were calculated either as the negative of the HOMO energy¹² (IP_{HOMO} ; Koopman's theorem) or as the difference in total energy between the molecule and its cation (ΔSCF), but since these two different methods of calculating the ionization potentials correlated well, only the IP_{HOMO} values were used in subsequent calculations. Solvent effects were not considered, notwithstanding their obvious importance, as for a series of similar compounds with E_{ox} measured under similar conditions, it can be assumed that trends in gas-phase ionization potentials correlate with solution-phase oxidation potentials.

In each case, the MNDO-PM3-optimized geometries are close to the X-ray structures with typical deviations of 0.01 Å. The trend in the bending angle of the TTF moiety is reproduced with the exception of 20, although the calculated bending in each case is larger than that observed experimentally. The correlation between calculated ionization potentials and experimentally determined oxidation potentials is of greater interest, and Table III shows that the ordering of all the cage molecules is predicted correctly by the calculations.

Having established that the MNDO-PM3 method is able to reproduce experimental trends, we performed some model calculations in order to obtain further insight into the variation of oxidation potentials with structure. Replacing the hydrogens in TTF with thiomethyl groups lowers the HOMO orbital energy, corresponding to an increase in oxidation potential, in line with previous results using the MNDO method and with experimental data.¹³ Bending the TTF molecule in analogy with that observed in the cage structures also increases the ionization potential since the HOMO becomes more localized on the central $C=C$ bond. Calculations performed on the face-to-face complex of TTF with benzene showed that the HOMO

(10) Stewart, J. J. P. *J. Comput. Chem.* 1989, 10, 209, 211.

(11) Baker, J.; Jensen, F.; Rzepac, H. S.; Stebbings, A. *QCPE Bulletin* 10, 1990, 76.

(12) Koopman, T. A. *Physica* 1933, 104.

(13) Bowadt, S.; Jensen, F. *Synth. Metals* 1989, 32, 179.

(14) (a) Malhotra, N.; Roepstorff, F.; Hansen, T. K.; Becher, J. *J. Am. Chem. Soc.* 1990, 112, 3709. (b) Christiansen, K.; Becher, J.; Hansen, T. K. *Tetrahedron Lett.* 1992, 33, 3035.

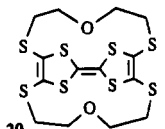
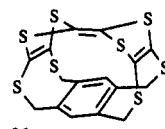
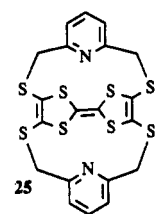
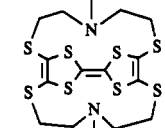
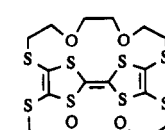
Table II. Selected Least-Squares Plane and Dihedral Angle Data for Externally Bridged TTF Structures 20,^a 21,^a 25,^b and 23^{c*}

(a) Deviations of Atoms (Å) from the Mean Plane through the Four S Atoms in the TTF System					
	20 ^a		21 ^a	25 ^b	23 ^c
	A	B			
S(1)	0.039(7)	-0.024(7)	0.003(1)	-0.002(2)	0.011(2)
S(3)	-0.038(7)	0.025(7)	-0.003(1)	0.002(2)	-0.011(2)
S(5)	-0.039(7)	0.025(6)	(-0.003)	0.002(2)	-0.011(2)
S(7)	0.038(6)	-0.025(6)	(0.003)	-0.002(2)	0.011(2)
C(1)	-0.213(23)	-0.169(21)	-0.053(3)	-0.200(3)	-0.178(4)
C(8)	-0.217(23)	-0.247(23)	(-0.053)	-0.177(3)	-0.145(4)
C(2)	1.163(25)	1.291(28)	0.902(3)	1.254(4)	1.269(5)
C(3)	1.202(28)	1.235(21)	0.894(3)	1.243(4)	1.238(5)
C(9)	1.224(25)	1.125(23)	(0.894)	1.140(4)	1.117(5)
C(10)	1.244(25)	1.192(23)	(0.902)	1.141(4)	1.137(5)
S(2)	2.310(8)	2.347(8)	1.659(1)	2.323(2)	2.427(2)
S(4)	2.304(8)	2.315(8)	1.625(1)	2.356(2)	2.357(2)
S(6)	2.379(7)	2.301(7)	(1.625)	2.176(2)	2.100(2)
S(8)	2.315(8)	2.394(7)	(1.659)	2.181(2)	2.172(2)

(b) Dihedral Angles (deg)					
angle between	20 ^a		21 ^a	25 ^b	23 ^c
	A	B			
line C(1)-C(8) and plane S(1)C(1)S(3)	11.1(5)	6.7(5)	3.2(3)	12.7(4)	11.6(3)
line C(1)-C(8) and plane S(5)C(8)S(7)	13.3(5)	17.6(6)	3.2 ^d	9.4(4)	7.2(3)
plane S(1)C(1)S(3) and plane S(1)C(2)C(3)S(3)	38.2(12)	42.7(11)	31.4(2)	39.3(5)	41.2(5)
plane S(1)C(2)C(3)S(3) and plane S(2)C(2)C(3)S(4)	3.0(6)	4.7(7)	3.1(1)	0.4(5)	2.5(4)
plane S(5)C(8)S(7) and plane S(5)C(9)C(10)S(7)	39.3(15)	36.4(13)	31.4 ^d	35.6(5)	36.3(5)
plane S(5)C(9)C(10)S(7) and plane S(6)C(9)C(10)S(8)	3.2(5)	4.5(6)	3.1 ^d	1.0(5)	0.8(5)

* The atom numbering used in this table follows that in molecule 20 (Figure 5a). ^a Present work. ^b Reference 2c. ^c Reference 2b. ^d Symmetry-dependent values.

Table III. Empirical Oxidation Potentials (E_{ox}) Compared to Calculated Ionization Potentials

	E_{ox} (V)	IP _{cage} (eV) ^a	Δ SCF (eV) ^a	IP _{TMT} (eV) ^a	Δ IP (eV) ^a	bend (deg) ^b	bend (deg) ^a	R_{S-X} (Å) ^a
	1.26 (irr.)	9.02	8.71	8.84	0.18	12.5	14.4	5.1
	1.09 (irr.)	8.91	8.51	8.98	-0.07	10.9	15.9	4.1
	0.27	8.68	8.27	8.91	-0.23	10.0	14.5	3.8
	0.95	8.74	8.42	8.75	-0.01	9.5	12.6	4.8
	0.41	8.74	8.37	8.50	0.24	3.1	7.4	4.6

^a Data obtained with the MNDO-PM3 method. ^b Data obtained from X-ray structures.

energy rises as the distance between the two π -systems decreases, with the effect becoming significant when the

distance falls below 4 Å. The first of these effects can thus be thought of as an inductive or through-bond effect,

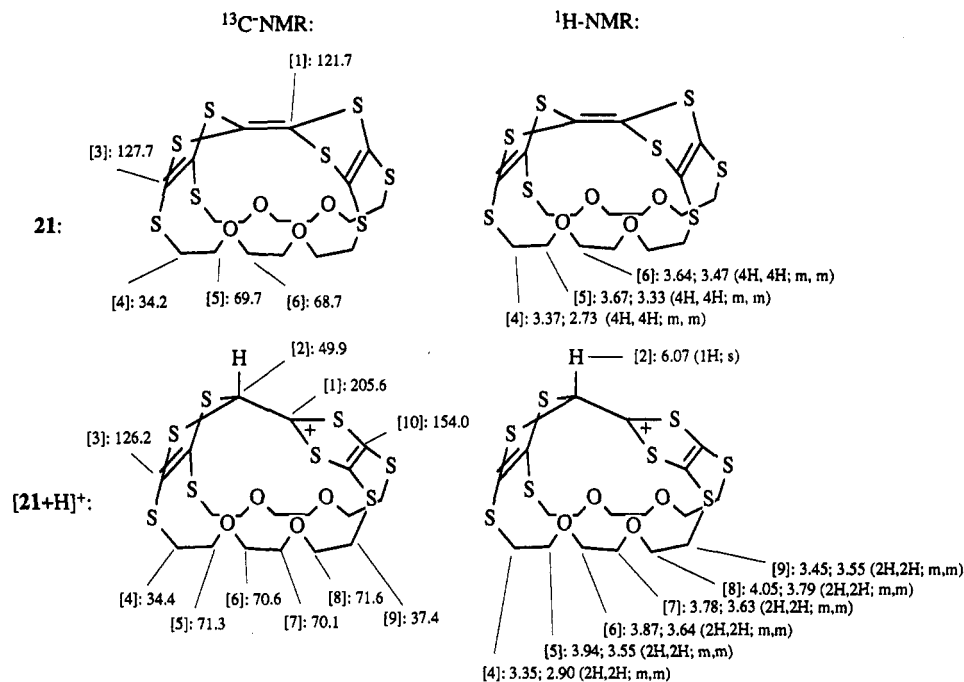


Figure 8.

the second as a HOMO localization due to bending, and the third as a through-space effect in which the electron-electron repulsion raises the HOMO energy. Table III also shows the calculated HOMO energies for the five cage compounds and for tetrathiomethyl TTF structures (IP_{TMT}) where the TTF geometry is taken to be the same as for the cages, and the differences are shown in the Δ IP column. The smallest distance between those sulfurs in the TTF moiety, which has the largest coefficients of the HOMO, and any hetero- or π -atom in the chain is denoted R_{S-X} in Table III. If **20** and **21** are compared, it is clear that IP_{cage} is lower than IP_{TMT} by a roughly constant 0.2 eV, an effect which can be designated as inductive. The amino chain in **23** should be less electron attracting than the corresponding ether system, and this is reflected in the smaller value of Δ IP. For the cages **26** and **25** we find that they are more easily oxidized than the thiomethyl analogs, and this correlates well with the fact that these two compounds also have the smallest distance between the TTF sulfur atoms and the aromatic systems in the chain.

In order to substantiate the through-space effect, we have performed calculations on systems with thiophene, furan, and pyrrole in the chain instead of pyridine as in **25**. The geometry for each of these systems is quite similar to that of the pyridine cage, and they also have lower oxidation potentials than the thiomethyl compounds. The calculated Δ IP is similar for the three compounds as expected from a roughly constant value of R_{S-X} . The calculations predict that the thiophene cage should have an oxidation potential slightly higher than that of the pyridino cage **25**, while the furan and pyrrole systems should resemble the diether cage **21**.

In the search for TTF compounds with low oxidation potentials, the above analysis suggests that this can be accomplished by forcing an aromatic system or the lone pairs of a heteroatom close (<4 Å) to the TTF π -system, while at the same time preventing bending of the TTF moiety. In the present cage compounds, the repulsion between the π -systems is relieved by bending the TTF part of the molecule, and the observed oxidation potentials

are a consequence of the energetic balancing of these two effects. If, however, the "chain" could be made sufficiently stiff and longer than the TTF molecule itself, it might be possible to achieve very low oxidation potentials. One such possibility might be to use anthracene or tetracene with sufficiently short connecting chains. It would also be of interest to know the experimental oxidation potential of **22**, which is predicted to be more easily oxidizable than the pyridino cage **25**.

The physicochemical properties of the new cages, in particular **21**, were investigated by various methods. The oxidation potentials (obtained by CV) listed in Table III have already been mentioned. In contrast to "normal" tetrathiafulvalenes, the present derivatives do not form complexes with TCNQ or DDQ. This could be due to the relatively high oxidation potentials in some cases or steric reasons in other instances.

The metal binding properties of **21**, investigated by the use of plasma desorption mass spectroscopy (PDMS), revealed that **21** possesses practically no affinity for alkali metal ions, very poor affinity for silver ions, and no affinity for Tl⁺. These data were confirmed by extraction experiments, in which the ligand **21** was unable to extract measurable amounts of alkali metal picrates into a chloroform phase.

Although these results were discouraging, we carried out an additional experiment which might prove important for future work. Müllens' work⁴ indicated the possibility of generating a stable cation by protonation of a TTF unit. In the case of **21** this can be visualized as a bowl-shaped unsymmetrical molecule with a positive charge at the bottom of the bowl. Substituting the ether functions with quaternary amines could turn the system into a potential anion binding compound. To test the stability of such a system, we performed NMR experiments on the model system **21**. Using ¹H-NMR, ¹³C-NMR, COSY, HETCOR,¹⁵ and HMBC¹⁶ techniques, we were able to

(15) (a) Bax, A. *J. Magn. Res.* 1983, 53, 517. (b) Rutar, V. *J. Magn. Res.* 1984, 58, 306. (c) Wilte, J. A.; Bolton, P. H. *J. Magn. Res.* 1984, 59, 343.

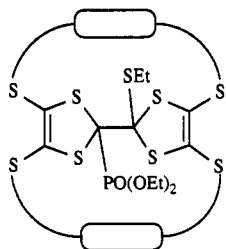


Figure 9.

study and fully assign the spectral data to the structure 21 and its protonated counterpart $[21 + H]^+$ as indicated in Figure 8.

The experiment was carried out in deuterated chloroform, and the spectra were run under increasingly acidic conditions created by the dropwise addition of trifluoroacetic acid directly into the NMR tubes, which turned the almost colorless solution a deep red.¹⁷ With 8–20 equiv of acid, extensive broadening of all proton signals compared to the unacidified spectrum was observed; however, at 40 equiv, the spectrum again displayed sharp signals allowing ¹³C- and 2D-experiments to be performed. The appearance of a sharp singlet at δ 6.07 which integrated as one proton compared to the rest of the spectrum, as well as the relatively simple ¹³C-NMR spectrum, were in full agreement with the structure in Figure 8 which was fully confirmed by the more sophisticated 2D experiments. It was not possible to obtain similar results with 23 because the protonated amines generated very broad signals.

Experimental Section

General. The CV experiments were all conducted in acetonitrile (0.1 M Bu₄NPF₆ as supporting electrolyte). Counter and working electrodes were made of platinum, and potentials were referenced versus SCE. Sweep rates in all experiments were 100 mV/s. For the NMR investigation standard pulse sequences were used. All NMR spectra were recorded in CDCl₃ with TMS as internal standard unless otherwise stated. Melting points are uncorrected. Elemental analyses were carried out by Microanalytical Lab, Copenhagen University. Solvents were dried by standard techniques.

Synthesis. Crown ether dimers 14–16 were obtained as described in the first part of this paper.³ **6:** 1,5-Dichloro-3-methyl-3-azapentane, Hydrochloride.¹⁸ **WARNING:** A mustard gas analog! Formic acid (10.0 g; 0.2 mol) and 37% formaldehyde (20 mL) were mixed in a 250-mL round-bottom flask equipped with a reflux condenser. 1,5-Dichloro-3-azapentane, hydrochloride (17.0 g; 0.1 mol) was added, and the solution heated with magnetic stirring at 100 °C. After 3 h the temperature was increased to 120 °C for 20 min and finally allowed to cool to room temperature before the solvent was evaporated in vacuo to afford the white solid 6 in quantitative yield. Due to the toxic nature of 6, no attempts to purify the compound further were made. ¹H-NMR (*d*₆-DMSO): 2.93 (3 H, s); 3.60 (4 H, t); 4.13 (4 H, t).

7: 1,5-Dichloro-3-ethyl-3-azapentane, Hydrochloride.¹⁹ **WARNING:** A mustard compound! *N*-Ethyl-2,2'-diethanolamine (20 g; 0.15 mol) dissolved in chloroform (50 mL) was placed in a round-bottom flask equipped with a stirrer, a dropping funnel, and a reflux condenser. Thionyl chloride (72 g; 0.6 mol) dissolved in chloroform (50 mL) was added slowly (4 h) with constant stirring. The pale yellow solution and white solid were refluxed for 4 h and cooled to room temperature. The solution was evaporated to dryness affording the product in quantitative yield. Due to the toxic nature of 7, no attempts to purify the compound

further were made. ¹H-NMR (*d*₆-DMSO): 1.26 (3 H, t); 3.27 (2 H, q); 3.52 (4 H, t); 4.07 (4 H).

17: 5,17-Dimethyl-2,8,10,12,14,20,22,24-octathia-5,17-diazatricyclo[19.3.0.0^{9,13}]tetracos-1(21),9(13)-diene-11,23-thione. **18:** 5,17-Diethyl-2,8,10,12,14,20,22,24-octathia-5,17-diazatricyclo[19.3.0.0^{9,13}]tetracos-1(21),9(13)-diene-11,23-thione. **General Procedure for Compounds 17 and 18.** Cesium carbonate (6.0 g; 0.02 mol) was suspended in dry DMF (500 mL) in a 1-L three-necked round-bottom flask under inert atmosphere. A solution of disodium 2-thioxo-1,3-dithiole-4,5-dithiolate, (made from 8.12 g (0.02 mol) of 4,5-bis(benzoylthio)-1,3-dithiole-2-thione⁵) in 50 mL of DMF was added simultaneously with a solution of 6 (4.0 g; 0.02 mol) or 7 (4.2 g; 0.02 mol) in 50 mL of DMF to the flask over 10 h, maintaining the addition of the two solutions at the same rate by the use of a medical Perfusor Pump. The temperature was then increased to 45 °C for 48 h. The precipitated salt was filtered off and washed with DMF, and the DMF fractions were combined. **Workup Procedure for 17.** The volume was reduced to ca. 70 mL on a rotary evaporator. After addition of a little dichloromethane the product precipitated. The product was washed with one 10-mL portion of dichloromethane and dried. The monomer 13 could be isolated from the mother liquor. **Workup Procedure for 18.** The solvent was removed on a rotary evaporator connected to an oil pump. The product was chromatographed (PTLC) on silica plates with petroleum ether (bp 65–70 °C)/dichloromethane (1:2) as eluent. The product appeared as the major yellow band and was extracted from the silica with ethyl acetate.

17. Yield: 1.01 g, 18%. Mp: 172–74 °C (toluene/MeOH). IR (KBr) ν (cm⁻¹): 1065 (C=S); PDMS (TFA): calcd mass 562.02, found 563.5 (MH⁺). ¹H-NMR: 2.31 (6 H, s); 2.77 (8 H, t); 3.07 (8 H, t). ¹³C-NMR: 34.96, 41.50, 55.87, 136.38, 210.98. Anal. Calcd for C₁₈H₂₂N₂S₁₀: C, 34.13; H, 3.94; N, 4.98, S, 56.95. Found: C, 34.73; H, 4.13; N, 5.03; S, 56.41.

18. Yield: 480 mg, 16%. Mp: 131–32 °C (CHCl₃/MeOH); IR (KBr) ν (cm⁻¹): 1063 (C=S); PDMS (TFA): calcd mass 591.07, found 591.7 (MH⁺). ¹H-NMR: 1.05 (6 H, t); 2.61 (4 H, q); 2.84 (8 H, t); 3.06 (8 H, t). Anal. Calcd for C₁₈H₂₆N₂S₁₀: C, 36.61; H, 4.41; N, 4.75, S, 54.24. Found: C, 36.21; H, 4.33; N, 4.70; S, 55.00.

19. Sodium (0.60 g, 26 mmol) was added to dry ethanol (45 mL), and the resulting solution of sodium ethoxide was added to a stirred suspension of 4,5-bis(benzoylthio)-1,3-dithiole-2-thione⁵ (4.1 g, 10.1 mmol) in dry ethanol (180 mL), under an argon atmosphere, at room temperature to give a deep red solution of the disodium salt 1. A solution of 2,6-bis(bromomethyl)pyridine (2.7 g, 10.1 mmole) in ethanol (100 mL) was added over 12 h and stirring continued for a further 6 h. The resulting yellow precipitate was filtered, washed with ethanol, and air dried to give the macrocyclic dimer 19 (2.9 g, 95%) as a yellow solid which could be recrystallized from chloroform. Mp: 84–86 °C. EI-MS: *m/z* 602 (M⁺, 0.5); 470 (1); 355 (1); 192 (2); 166 (5); 137 (4); 76 (100). PDMS: *m/z* 602 (100%). ¹H-NMR: 4.09 (8 H, s); 7.15 (4 H, d); 7.65 (2 H, t). IR (KBr): (cm⁻¹) 3058, 1629, 1589, 1572, 1453, 1064, 1038. Anal. Calcd for C₂₀H₁₄N₂S₁₀: C, 39.86; H, 2.33; N, 4.65. Found: C, 39.83; H, 2.37; N, 4.85.

20: 1,4,5,6-Tetrahydro-2,7,3,6-bis(4-oxa-1,7-dithiaheptane-1,7-diyl)-1,4,5,8-tetrathiafulvalene. **21:** 1,4,5,6-Tetrahydro-2,7,3,6-bis(4,7-dioxa-1,10-dithiadecane-1,10-diyl)-1,4,5,8-tetrathiafulvalene. **23:** 1,4,5,6-Tetrahydro-2,7,3,6-bis(4-methyl-4-aza-1,7-dithiaheptane-1,7-diyl)-1,4,5,8-tetrathiafulvalene. **24:** 1,4,5,6-Tetrahydro-2,7,3,6-bis(4-ethyl-4-aza-1,7-dithiaheptane-1,7-diyl)-1,4,5,8-tetrathiafulvalene. **25:** 1,4,5,6-Tetrahydro-2,7,3,6-bis(2',6'-pyridylenebismethylene)-1,4,5,8-tetrathiafulvalene. **General Procedure for 20, 21, 23, 24, and 25.** To a solution of either 14 (640 mg), 15 (750 mg), 17 (600 mg), or 18 (600 mg) in dry xylene (15 mL) was added freshly distilled triethyl phosphite (2 mL), and the mixture was refluxed under argon for 5 h in the case of 14 and 15, whereas 45 min was sufficient in the case of 17 and 18. The reddish-orange solution was cooled and xylene was distilled off under reduced pressure. 20 or 21 separated as light amber solids. Compound 21 was recrystallized by dissolving it in chloroform and reprecipitated by slow diffusion of a layer of methanol into the chloroform layer. Compound 20 was recrystallized using a similar procedure but with methylene chloride and methanol as the solvent system. These methods afforded crystals of a size and quality allowing X-ray crystal-

(16) Bax, A.; Summers, M. F. *J. Am. Chem. Soc.* 1986, 108, 2093.

(17) The development of red color was reversible and disappeared immediately on addition of triethylamine, even after a week, indicating the cation to be fairly stable.

(18) Worrell, J. H.; Jackman, T. A. *Inorg. Chem.* 1978, 17, 3358.

(19) Hanby, W. E.; Rydon, H. N. *J. Chem. Soc.* 1947, 517.

lography to be performed. Compound 19 (100 mg) and 1 mL of triethyl phosphite in xylene (30 mL) were refluxed for 3 h and cooled, and the precipitated 25 was collected and recrystallized from methylene chloride.

20. Yield: 108 mg (19%). Mp: >270 °C dec. MS: m/z 472 (M^+ , 100); 368 (10); 264 (19); 88 (60). $^1\text{H-NMR}$: 3.98 (4 H, m); 3.36 (4 H, m); 3.06 (4 H, m); 2.74 (4 H, m). $^{13}\text{C-NMR}$: 134.89; 132.52; 71.04; 35.51. IR (cm^{-1}): 1631, 1070. Anal. Calcd for $\text{C}_{14}\text{H}_{16}\text{O}_2\text{S}_8\text{H}_2\text{O}$: C, 34.28; H, 3.67. Found: C, 34.07; H, 3.39.

21. Yield: 155 mg (23%). Mp: 247 °C. MS: m/z 560 (M^+ , 100); 262 (3); 224 (3); 45 (10). $^1\text{H-NMR}$: 3.66 (8 H, m); 3.49 (4 H, m); 3.37 (8 H, m); 2.73 (4 H, m). $^{13}\text{C-NMR}$: 127.5; 121.6; 69.6; 68.6; 34.1. IR (cm^{-1}): 1132. UV: (CHCl_3) λ_{max} 338 (3.16); 304 (2.73); 259 (3.15). Anal. Calcd for $\text{C}_{18}\text{H}_{24}\text{O}_4\text{S}_8$: C, 38.55; H, 4.31. Found: C, 38.65; H, 4.30.

23. Yield: 100 mg (22%). Mp: 237–38 °C dec ($\text{CHCl}_3/\text{MeOH}$). IR (KBr) ν (cm^{-1}): 1044. MS: m/e 498 (M^+ , 81). $^1\text{H-NMR}$: 2.25 (6 H, s); 2.31 (4 H, m); 2.67 (8 H, m); 3.27 (4 H, m). Anal. Calcd for $\text{C}_{16}\text{H}_{22}\text{N}_2\text{S}_8$: C, 38.55; H, 4.42; N, 5.62. Found: C, 38.40; H, 4.45; N, 5.44.

24. Yield: 125 mg (23%). Mp: 203–4 °C (ether/ CHCl_3); IR: (KBr) ν (cm^{-1}): 1060 (C=S). MS: m/e 526 (M^+ , 31%). $^1\text{H-NMR}$: 1.05 (6 H, q); 2.29 (4 H, hex); 2.52 (4 H, t); 2.64 (4 H, hex); 2.83 (4 H, hex); 3.26 (4 H, hex). Anal. Calcd for $\text{C}_{18}\text{H}_{26}\text{N}_2\text{S}_8$: C, 41.06; H, 4.94; N, 5.32. Found: C, 40.92; H, 4.80; N, 5.22.

25. Yield: 20 mg (20%). Mp: 290–92 °C; MS: m/z 538 (M^+ , 100). $^1\text{H-NMR}$: 3.85 (4 H, d); 4.16 (4 H, d); 7.47 (4 H, d); 7.77 (2 H, t). IR (KBr) (cm^{-1}): 2976, 2922, 1631, 1589, 1572, 1451. UV: (CHCl_3) λ_{max} 240 (4.21); 262 (4.22); 340 (3.85). Anal. Calcd for $\text{C}_{20}\text{H}_{14}\text{N}_2\text{S}_8$: C, 5.20; H, 2.60; N, 5.20. Found: C, 44.54; H, 2.60; N, 5.14.

29: 4,5-Bis[(2'-hydroxyethyl)thio]-1,3-dithiole-2-thione.⁸ A solution of sodium (1.20 g; 0.052 mol) in 40 mL of dry ethanol was added to a suspension of 8.12 g (0.02 mol) of 4,5-bis-(benzoylthio)-1,3-dithiole-2-thione⁵ in 80 mL of dry ethanol under nitrogen. When all of the solid material was dissolved (15–30 min), 2-chloroethanol (10 mL, excess) was added in one portion. The following day the ethanol was evaporated off, and 150 mL of ethyl acetate was added. The yellow solution was filtered and reduced to half the initial volume in vacuo, and petroleum ether (bp 65–70 °C) was added until the solution became turbid. Cooling in a refrigerator overnight completed the crystallization, and 4.65 g (81%) of yellow plates was filtered off.

29. MS: m/z 286 (M^+ , 100), 242 (4); 165 (9); 121 (24); 88 (30). IR: (KBr): 3290, 1069. $^1\text{H-NMR}$: 3.05 (4 H, t, $J = 6$ Hz), 3.63 (4 H, q, $J = 6$ Hz), 5.06 (2 H, t, $J = 6$ Hz). $^{13}\text{C-NMR}$: 210.7; 136.0; 60.0; 59.9. Anal. Calcd for $\text{C}_7\text{H}_{10}\text{O}_2\text{S}_5$: C, 29.37; H, 3.50, S, 55.94. Found: C, 29.55; H, 3.53; S, 55.55.

30: 4,5-Bis[(2'-tosylethyl)thio]-1,3-dithiole-2-thione. To a solution of 29 (2.48 g; 0.01 mol) in 50 mL of dry pyridine was added 4.0 g (0.03 mol) of tosyl chloride, and the mixture was stirred overnight. The following day pyridine was removed in vacuo, and 50 mL water was added. The compound was extracted with 3 × 50 mL of chloroform, and the chloroform phase was dried with MgSO_4 (anhyd) and evaporated in vacuo, leaving 4.34 g (73%) of a heavy yellow oil 30 that was best converted directly to 31. 30. MS: m/z 594 (M^+ , 1.2); 458 (59), 224 (41), 155 (90), 91 (100). IR: (cm^{-1}) 1598, 1360, 1061. $^1\text{H-NMR}$: 2.46 (6 H, s); 3.08 (4 H, t), 4.19 (4 H, t); 7.37 (4 H, d); 7.78 (4 H, d). $^{13}\text{C-NMR}$: 209.7; 145.5; 136.0; 132.4; 130.1; 128.0; 67.5; 35.0; 21.8.

31: 4,5-Bis[(2'-bromoethyl)thio]-1,3-dithiole-2-thione. A mixture of 30 (5.0 g; 0.085 mol) and LiBr (5 g) was refluxed in acetone for 5 h. The solvent was removed in vacuo and the residue redissolved in the minimum amount of chloroform and filtered through silica. The chloroform was removed in vacuo, and the remaining solid was recrystallized from chloroform/methanol to give 3.40 g (78%) of yellow needles. The compound crystallized with half a mol of methanol. 31. Mp: 55–56 °C. MS: m/z 412

(M^+ , 1), 348 (19), 304 (22), 165 (11), 121 (24); 88 (51); 46 (100). IR (cm^{-1}): 1057. $^1\text{H-NMR}$: 3.35 (4 H, t); 3.65 (4 H, t). Anal. Calcd for $(\text{C}_7\text{H}_6\text{S}_5\text{Br}_2)_2\text{CH}_3\text{OH}$: C, 21.43; H, 2.40. Found: C, 21.35; H, 2.02.

32: 4,5-Bis(vinylthio)-1,3-dithiole-2-thione. To a solution of 1.2 g of 31 in THF (50 mL) was added sodium ethoxide (0.5 g) dissolved in dry ethanol (25 mL), and the mixture was stirred at room temperature overnight. After evaporation of the solvent in vacuo the mixture was separated by preparative layer chromatography using methylene chloride/petroleum ether (1:1) as eluent. The top yellow band was extracted, leaving a yellow-orange oil 32.

32. Yield: 0.28 g (38%); MS: m/z 250 (M^+ , 79), 234, (11), 173 (9), 103 (38), 88 (37), 71 (100). IR (KBr) ν (cm^{-1}): 1043. $^1\text{H-NMR}$ (60 MHz): 6.3 (2 H, dd, $J_a = 7$ Hz; $J_b = 15$ Hz); 5.3 (2 H, d, $J = 15$ Hz); 5.4 (2 H, d, $J = 7$ Hz).

33: Tetrahydrotetrafulvalene. 31 (220 mg; 0.5 mmol) and *N,N*-dimethyl-1,2-diaminoethane (90 mg; 1 mmol) were dissolved in dry xylene (10 mL) and stirred under nitrogen for 24 h. After evaporation of the solvent, the residue was dissolved in the minimum amount of dichloromethane, and petroleum ether was added until crystallization began. The product was filtered, washed with petroleum ether, and dried. Yield: 40 mg (38%). Mp: 172–74 °C (lit.²⁰ 200–2 °C). IR (KBr) cm^{-1} : 1196. MS m/e 208 (M^+ , 100). $^1\text{H-NMR}$: 3.35 (8 H, s).

X-ray Crystallography. The X-ray measurements were carried out on crystals mounted on glass fibers using an Enraf-Nonius CAD4 diffractometer and graphite-monochromated Mo $K\alpha$ radiation ($\lambda = 0.71069 \text{ \AA}$). The single specimen of 20 was obtained with difficulty, being cut from a larger, comprehensively twinned, cluster. Following SEARCH and INDEX procedures, improved orientation matrices and cell dimensions were obtained by refinement of the setting angles for 25 well-distributed reflections with $10 < \theta < 13^\circ$. For the sample of 20, peak width showed considerable variation. Intensity data were collected via the $\omega/2\theta$ scan mode following normal procedures²¹ and corrected for Lorentz and polarization effects, but not for absorption. The data for 20 were also corrected for the 3% linear fall in the intensities of the standard reflections during collection. The crystal for 21 showed only minor fluctuations in the standard intensities. The structures were solved using direct methods (SHELXS)²² and refined by full-matrix least-squares (SHELX-80).²³ In both cases the non-hydrogen atoms were refined anisotropically [except C(1) in molecule B of 20, which was kept isotropic because attempts to refine it anisotropically gave nonpositive definite temperature factor coefficients]. The hydrogens were included in idealised positions (CH = 0.96 Å) with a common Uiso for all in 20, but their positional and isotropic thermal parameters were freely refined in 21. Crystal data and other experimental details are given elsewhere. The author has deposited atomic coordinates with the Cambridge Crystallographic Centre. The coordinates can be obtained, on request, from the Director, Cambridge Crystallographic Centre, 12 Union Road, Cambridge, CB2 1EZ, UK. Sources of scattering factors are as in ref 23.

Acknowledgment. We warmly thank the Danish Research Councils (STVF and SNF) for financial support to TKH and Forskerakademiet for a travel grant to B.G.

(20) Coffen, D. L.; Garrett, P. E. *Tetrahedron Lett.* 1969, 2043.

(21) Jones, R. A.; Malik, K. M. A.; Hursthouse, M. B.; Wilkinson, G. *J. Am. Chem. Soc.* 1979, 101, 4128.

(22) Sheldrick, G. M. SHELXS Program for Crystal Structure Solution, University of Göttingen, 1986.

(23) Sheldrick, G. M. SHELX-80 Program for Crystal Structure Solution and Refinement, University of Göttingen, 1980.